Coarse-graining intermittent intracellular transport: Two- and three-dimensional models

Sean D. Lawley,* Marie Tuft, and Heather A. Brooks
Department of Mathematics, University of Utah, Salt Lake City, Utah 84112, USA
(Received 31 August 2015; published 20 October 2015)

Viruses and other cellular cargo that lack locomotion must rely on diffusion and cellular transport systems to navigate through a biological cell. Indeed, advances in single particle tracking have revealed that viral motion alternates between (a) diffusion in the cytoplasm and (b) active transport along microtubules. This intermittency makes quantitative analysis of trajectories difficult. Therefore, the purpose of this paper is to construct mathematical methods to approximate intermittent dynamics by effective stochastic differential equations. The coarse-graining method that we develop is more accurate than existing techniques and applicable to a wide range of intermittent transport models. In particular, we apply our method to two- and three-dimensional cell geometries (disk, sphere, and cylinder) and demonstrate its accuracy. In addition to these specific applications, we also explain our method in full generality for use on future intermittent models.

DOI: 10.1103/PhysRevE.92.042709 PACS number(s): 87.17.Aa, 87.16.A−, 05.10.Gg, 87.10.−e

I. INTRODUCTION

Intracellular transport of cargo (macromolecules and organelles) is fundamental to cellular function. Indeed, many diseases are associated with defects in intracellular transport [1]. In addition, trafficking through the cytoplasm is a crucial step in viral and nonviral mediated gene transfer [2–4]. In order to infect and multiply inside a host cell, viruses must travel through the cytoplasm to the nucleus, and newly formed viral progeny must travel back this route to exit the cell.

Lacking locomotion, viruses and other cellular cargo must rely on diffusion and existing cellular transport systems to maneuver through a biological cell. Advances in live cell imaging and single particle tracking have revealed the complex nature of viral motion. Viruses alternate between epochs of (a) diffusion in the cytoplasm and (b) active transport along microtubules [5–7]. This intermittency makes quantitative analysis of trajectories difficult.

Therefore, we seek to approximate the intermittent dynamics by some simpler effective dynamics. In this paper, we answer the following question: given information about the cell and the cargo (cellular and microtubular geometry, cargo dynamics in cytoplasm, cargo dynamics on microtubules, number of microtubules, etc.), how can we find an effective stochastic differential equation (SDE) to approximate the intermittent cargo motion? Put another way, we show how to choose two parameters (the drift and diffusion coefficient in an SDE) that encapsulate the full intermittent dynamics.

Using Monte Carlo simulations, we verify the accuracy of our methods by showing that the probability distributions of random variables stemming from our effective SDE match the probability distributions of random variables stemming from the full intermittent process. In particular, we compare the distributions of first passage times (FPTs) and the distributions of the spatial position of the process at a sequence of times. We note that this is a more stringent test of accuracy than previous methods which sought to match only *means* of FPTs and not *distributions* of FPTs [8,9].

Given its biological and medical importance, intracellular transport has garnered mathematical attention for decades [10]. Recently, mathematicians have developed techniques to compute the efficiency of the delivery of plasmids or viral DNAs from the cell membrane to nuclear pores [11–13]. These techniques, however, take as their starting point a single SDE describing cargo motion, not the full intermittent dynamics. Our method for reducing intermittent dynamics to an SDE is therefore well motivated. Existing methods for this reduction exist, but they apply only to two-dimensional cells [8,9]. Our method applies to three-dimensional cells (Secs. IV and V) and is in fact more accurate than previous methods for two-dimensional cells (Sec. II).

The paper is organized as follows. We begin in Sec. II by describing a well-known model of intermittent intracellular transport in a two-dimensional cell that was first formulated in Ref. [8]. In Refs. [8,9], the authors derive effective SDEs to approximate this intermittent model, and so we compare our coarse-graining method to theirs. We give our general coarse-graining method in Sec. III and demonstrate its wide applicability in Secs. IV and V by applying it to models of intermittent intracellular transport in spherical and cylindrical cellular geometries, respectively. In all cases, Monte Carlo simulations show that our effective SDE closely resembles the intermittent dynamics. We conclude with a brief summary.

II. TWO-DIMENSIONAL CELL—DISK

We begin by applying our coarse-graining method to a well-known model of virus trafficking in a two-dimensional cell that was formulated in Ref. [8] and further studied in Refs. [9,12]. In this model, the cell is a two-dimensional disk of radius R with its nucleus located in a concentric disk of smaller radius $\delta < R$ (this cellular geometry would apply, for example, to flat skin fibroblast culture cells [14]). There are N microtubules radiating from the nucleus to the cellular membrane that partition the cytoplasm into N wedges of equal angular width $\Theta = 2\pi/N$ (see Fig. 1). By this symmetry, it is enough to consider the viral motion restricted to one of these N wedges:

$$C := \{(r,\theta) : \delta \leqslant r \leqslant R \text{ and } \theta \in [0,\Theta]\}.$$

*lawley@math.utah.edu

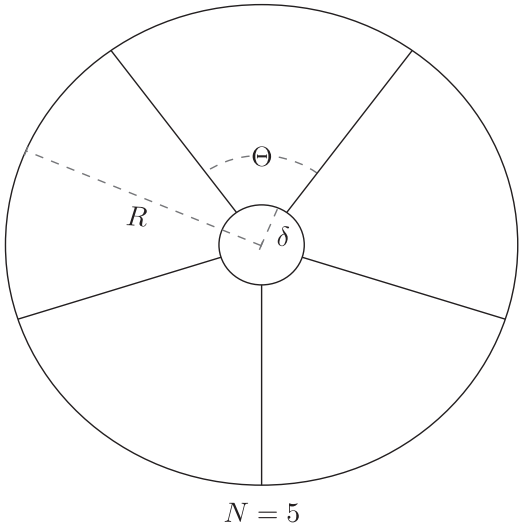

FIG. 1. Two-dimensional cell model with cell radius R, nucleus radius δ, and $N = 5$ microtubules. Each wedge has angular width $\Theta = 2\pi/N$.

A virus enters C at the cellular membrane at radius R at an angle uniformly distributed in $[0,\Theta]$. The virus then moves by pure diffusion with diffusion coefficient D in the cytoplasm (with a reflecting boundary condition at the cellular membrane at radius R) until it either hits the nucleus at radius δ or hits a microtubule at angle 0 or Θ. If the virus ever reaches radius δ, then it is immediately absorbed. If the virus hits a microtubule, then it moves along the microtubule toward the nucleus with constant velocity V for an exponentially distributed amount of time. After this exponential time, the virus is released back into the cytoplasm at its current radius at an angle uniformly distributed in $[0,\Theta]$ and begins to diffuse again (see Fig. 2).

The virus continues to alternate between epochs of diffusion and directed motion along microtubules until it reaches the nucleus. If we write the position of the virus at time t in polar coordinates $(r_t,\theta_t) \in C$, then viral motion is described by

$$dr_t = \begin{cases} -V\,dt & \text{on a microtubule} \\ (D/r_t)dt + \sqrt{2D}\,dW_t^r & \text{in cytoplasm,} \end{cases}$$
$$d\theta_t = \begin{cases} 0 & \text{on a microtubule} \\ (\sqrt{2D}/r_t)dW_t^\theta & \text{in cytoplasm,} \end{cases} \tag{2.1}$$

where W_t^r and W_t^θ are independent standard Brownian motions.

The intermittent nature of this process makes it difficult to analyze. Thus, much effort has gone into finding effective coarse-grained SDE approximations. In Sec. II A below, we outline this previous work and identify aspects that we seek to improve. We then give our coarse-grained SDE in Sec. II B and make comparisons in Sec. II C.

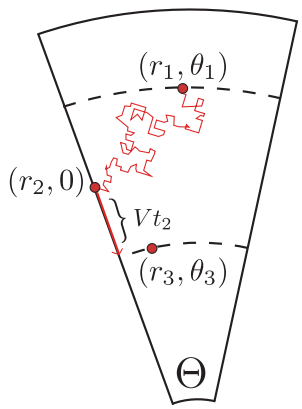

FIG. 2. (Color online) Sample trajectory of intermittent dynamics within a single wedge of two-dimensional cell model. Here, the virus diffuses in the cytoplasm from radius r_1 and angle θ_1 until it hits the microtubule at radius r_2 and angle 0. It then moves along the microtubule at velocity V for an exponentially distributed time t_2. Then, it is released back into the cytoplasm at radius $r_3 = r_2 - Vt_2$ and at an angle θ_3 uniformly distributed in $[0,\Theta]$. The process continues until the virus is absorbed at radius δ.

A. Previous coarse-grained dynamics by Lagache and Holcman

In Refs. [8,9], the authors use sophisticated asymptotic analysis of partial differential equations to derive a radial drift $B(r)$ in terms of model parameters in order to approximate the intermittent dynamics in Eq. (2.1) by an effective radial SDE

$$dr_t = [D/r_t - B(r_t)]\,dt + \sqrt{2D}\,dW_t. \tag{2.2}$$

In Ref. [8] the derived drift $B(r)$ is constant in r, whereas in Ref. [9] it a function of r. In both papers, the authors take the effective angular SDE to be the cytoplasmic angular SDE from the intermittent dynamics, namely,

$$d\theta_t = (\sqrt{2D}/r_t)\,dW_t^\theta.$$

In both Refs. [8,9], the approximation in Eq. (2.2) is justified by two criteria: (a) the mean first passage time (MFPT) to the nucleus for the effective dynamics in Eq. (2.2) closely matches the MFPT to the nucleus for the intermittent dynamics in Eq. (2.1) if $\Theta \ll 1$, and (b) if one imposes reflecting boundary conditions at the nucleus, then the steady state radial distribution of the effective dynamics in Eq. (2.2) resembles the steady state distribution of the intermittent dynamics in Eq. (2.1) for certain intermediate values of Θ.

The FPT to the nucleus is closely related to the probability and timing of viral infection and is thus a key biological quantity. Therefore, matching the FPTs for the two processes is a good criteria for justifying the coarse-grained SDE, and so we agree in principle with criteria (a). However, while the MFPTs for Eqs. (2.1) and (2.2) match closely, we discover below that the FPT *distributions* for the two processes are quite different. We thus seek an effective SDE whose FPT distribution matches that of the intermittent dynamics in Eq. (2.1). Furthermore, we want the effective SDE to be valid for a larger range of Θ. We see below that our effective SDE accomplishes both of these.

In addition, the criteria (b) of matching steady state radial distributions could be sharpened since steady state distributions contain (in principle) little information about time scale. As a trivial example, consider a diffusing particle in a one-dimensional interval with reflecting boundaries. The steady state distribution (uniform) is completely independent of the diffusion coefficient, but the dynamics are of course highly dependent on the diffusion coefficient. Instead of seeking to match the steady state radial distribution (which

is essentially the radial distribution at infinite time), we match the radial distribution at a sequence of finite times.

Furthermore, the fact that criteria (b) can only hold in certain intermediate parameter regimes is made clear by the form of the effective SDE in Eq. (2.2). Notice that the diffusion term in Eq. (2.2) is the same as the cytoplasmic diffusion term for the radial dynamics in Eq. (2.1). Thus, the effective SDE (2.2) always has this same amount of noise. However, this effective SDE was derived under the assumption that $\Theta \ll 1$, and it is clear that the intermittent process becomes deterministic in this limit because the proportion of time that the virus is bound to a microtubule converges to one. Thus, the steady state radial distribution for the intermittent process in this limit must be a delta function at the nucleus, and so the steady state radial distributions of Eqs. (2.1) and (2.2) cannot match in this limit. We see below that assuming the diffusion term in the effective SDE is the same as the cytoplasmic diffusion term causes other problems. We thus allow the diffusion term in our effective SDE to depend on Θ.

B. New coarse-grained dynamics

A systematic exposition of our general coarse-graining method is given below in Sec. III, but we first illustrate our method for the two-dimensional cell model described above. We approximate the intermittent dynamics of Eq. (2.1) by an effective radial SDE that is a mixture of the cytoplasmic and microtubular dynamics

$$dr_t = \{[D/r_t)(1 - p(r_t)] - Vp(r_t)\}dt + \sqrt{2D[1 - p(r_t)]}\,dW_t, \tag{2.3}$$

where $p(r)$ is related to the probability that the virus is on a microtubule given that it is at radius r.

A precise definition of $p(r)$ is given in Sec. III, but first consider the following intuitive derivation. By assumption, each time the virus hits a microtubule, it attaches to the microtubule for an exponential amount of time (say with mean μ). After this exponential time, the virus is released back into the cytoplasm at its current radius (call it r) at an angle uniformly distributed in $[0,\Theta]$. Ignoring radial motion, we approximate the amount of time it takes the virus to reach a microtubule again by

$$T(r) := \frac{1}{\Theta}\int_0^\Theta \tau(\theta; r)d\theta, \tag{2.4}$$

where $\tau(\theta; r)$ satisfies boundary value problem

$$\frac{D}{r^2}\frac{d}{d\theta}\tau(\theta; r) = -1, \quad \tau(0; r) = 0 = \tau(\Theta; r). \tag{2.5}$$

For a particle diffusing in the interval $[0,\Theta]$ with diffusion coefficient D/r^2, the quantity $T(r)$ is the MFPT to reach either 0 or Θ, given a uniform initial position [15]. A quick calculation yields $T(r) = \Theta^2 r^2/(12D)$.

Setting $p(r)$ as the proportion of time on a microtubule

$$p(r) = \frac{\mu}{\mu + T(r)},$$

our effective SDE in Eq. (2.3) becomes

$$dr_t = \left(\frac{D}{r_t}\frac{T(r_t)}{\mu + T(r_t)} - V\frac{\mu}{\mu + T(r_t)}\right)dt \times \sqrt{2D\frac{T(r_t)}{\mu + T(r_t)}}\,dW_t. \tag{2.6}$$

C. Comparison

We now compare our effective SDE in Eq. (2.6) to both the original intermittent process in Eq. (2.1) and the effective SDE in Eq. (2.2) derived in Ref. [9]. In keeping with parameter values used in Refs. [8,9] (taken from experimental papers [5,16–18]), we take the radius of the cell to be $R = 20\ \mu$m, the radius of the nucleus to be $\delta = 5\ \mu$m, the cytoplasmic diffusion coefficient to be $D = 1.3\ \mu\text{m}^2\,\text{s}^{-1}$, the velocity on microtubules to be $V = 0.7\ \mu\text{m}\,\text{s}^{-1}$, and the average time on a microtubule to be $\mu = 1$ s.

Figure 3 compares the distributions of the FPT to the nucleus for various numbers of microtubules ($N = 12,24,48,96$). These values of N are in keeping with [8,9] which used N between 12 and 48. Figure 4 compares the distributions of the radial positions at times $t = 5,10,15$ for $N = 48$. That is, it compares the distribution of r_t for (2.1), (2.6), and (2.2) at $t = 5,10,15$. The standard Euler-Maruyama method is used to simulate the cytoplasmic motion in the intermittent process as well as the effective SDEs. It is clear from these figures that our SDE in Eq. (2.6) approximates the intermittent process more closely than the SDE in Eq. (2.2) derived in Ref. [9].

III. GENERAL METHOD

Before considering higher dimensional and more complicated cellular geometries in Secs. IV and V, we first give our general coarse-graining method. Suppose one is given a stochastic process $\{(\rho_t,\phi_t)\}_{t\geqslant 0} \in \mathbb{R}\times\mathbb{R}^d$. [We use the (ρ,ϕ) notation for analogy to Sec. II above, but notice that (ρ,ϕ) is not assumed to be a radius and angle as it takes values in $\mathbb{R}\times\mathbb{R}^d$.]

Let the sets $\{A_k\}_{k=1}^n \subset \mathbb{R}^d$ partition the state space of ϕ_t and suppose the dynamics of ρ_t depend only on which A_k the process ϕ_t is in and not on the details of ϕ_t. That is, suppose the dynamics of ρ_t are governed by the SDE

$$d\rho_t = \left(\sum_{k=1}^n b_k(\rho_t)1_{\phi_t\in A_k}\right)dt + \left(\sum_{k=1}^n \sigma_k(\rho_t)1_{\phi_t\in A_k}\right)dW_t, \tag{3.1}$$

where $1_{\{\cdot\}}$ denotes the indicator function, for some given functions $\{b_k(\rho)\}_{k=1}^n$ and $\{\sigma_k(\rho)\}_{k=1}^n$. [In the case of the two-dimensional cell considered in Sec. II above, $\rho_t = r_t$, $\phi_t = \theta_t$, $b_1(\rho) = V$, $\sigma_1(\rho) = 0$, $b_2(\rho) = D/\rho$, and $\sigma_2(\rho) = \sqrt{2D}$, with partitioning sets $A_1 = \{0,\Theta\}$ and $A_2 = (0,\Theta)$.]

The dynamics of ϕ_t may be complicated and may depend on ρ_t, but we suppose that which set A_k the process ϕ_t is in is approximately Markovian. That is, we suppose there exists a continuous-time Markov jump process J_t (with instantaneous

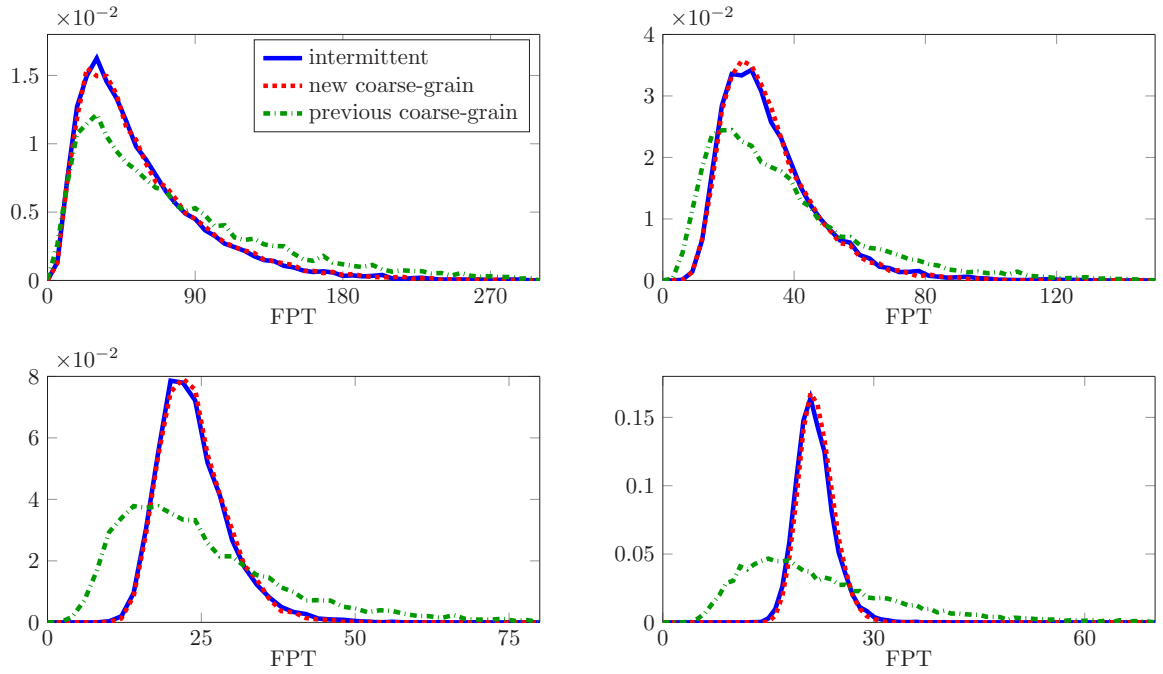

FIG. 3. (Color online) Empirical distributions of FPT to nucleus of 2D cell for intermittent in Eq. (2.1), our new coarse grain in Eq. (2.6), and the previous coarse grain in Eq. (2.2) derived in Ref. [9] for $N = 12$ (top left), $N = 24$ (top right), $N = 48$ (bottom left), and $N = 96$ (bottom right). Each distribution is calculated from 10^4 trials. Parameters are given in Sec. II C.

jump rates which may depend on ρ_t) so that

$$J_t \approx \sum_{k=1} k 1_{\phi_t \in A_k}.$$

[In the case of the two-dimensional cell considered in Sec. II above, J_t jumps from state 1 to 2 with rate $1/\mu$ and from 2 to 1 with rate $1/T(\rho_t)$.]

Under this assumption, we approximate ρ_t by

$$d\tilde{\rho}_t = \left(\sum_{k=1}^{n} b_k(\tilde{\rho}_t) 1_{J_t=k}\right) dt + \left(\sum_{k=1}^{n} \sigma_k(\tilde{\rho}_t) 1_{J_t=k}\right) dW_t.$$

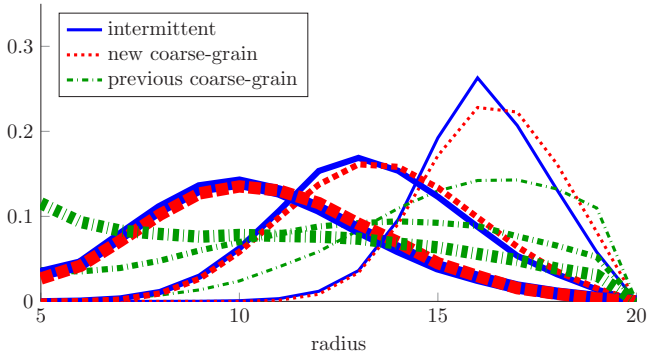

FIG. 4. (Color online) Empirical distribution of radial position for 2D cell for intermittent in Eq. (2.1), our new coarse grain in Eq. (2.6), and the previous coarse grain in Eq. (2.2) derived in Ref. [9] at times $t = 5, 10, 15$. Thicker lines correspond to larger times. Each distribution is calculated from 10^5 trials and we take $N = 48$. Parameters are given in Sec. II C.

This process $\tilde{\rho}_t$ is a hybrid switching diffusion [19]. If the J_t dynamics are much faster than the $\tilde{\rho}_t$ dynamics, then one can approximate $\tilde{\rho}_t$ to first order by the adiabatic limit (see Ref. [19], Chap. 12)

$$d\bar{\rho}_t = \left(\sum_{k=1}^{n} b_k(\bar{\rho}_t) p_k(\bar{\rho}_t)\right) dt + \left(\sum_{k=1}^{n} \sqrt{\sigma_k^2(\bar{\rho}_t) p_k(\bar{\rho}_t)}\right) dW_t, \tag{3.2}$$

where $\{p_k(\rho)\}_{k=1}^n$ is the quasi steady state distribution of J_t. This time scale separation is the key assumption. The SDE in Eq (3.2) is our coarse-grained effective SDE approximation to Eq. (3.1).

IV. THREE-DIMENSIONAL CELL—SPHERE

In this section, we first formulate a mathematical model of intermittent virus trafficking in a three-dimensional spherical cell and then apply our general coarse-graining method of Sec. III to derive an effective SDE describing viral motion.

In this intermittent model, the cell is a sphere of radius R with its nucleus located in a concentric sphere of smaller radius $\delta < R$. The position of the virus is restricted to the cytoplasm

$$C := \{\mathbf{x} \in \mathbb{R}^3 : |\mathbf{x}| \geqslant \delta \text{ and } |\mathbf{x}| \leqslant R\}.$$

There are N microtubules, each of radius ε, that radiate from the nucleus at radius δ to the cellular membrane at radius R (see Fig. 5). That is, for N points $\{\mathbf{c}_k\}_{k=1}^N$ on the unit sphere, we define the microtubules $\{m_k\}_{k=1}^N$ to be the sets

$$m_k = \{\mathbf{x} \in \mathbb{R}^3 : |\mathbf{x} - r\mathbf{c}_k| \leqslant \varepsilon \quad \text{for some} \quad r \in [\delta, R]\}.$$

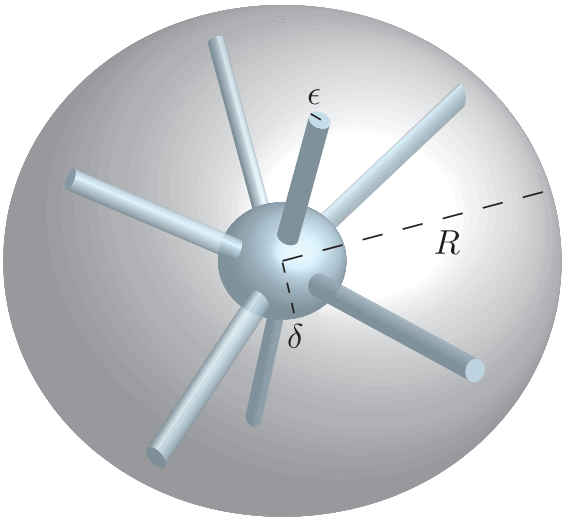

FIG. 5. (Color online) Three-dimensional spherical cell model with cell radius R, nucleus radius δ, and $N = 7$ microtubules with radius ε. The N microtubules radiate from locations on the nucleus which are randomly drawn from a uniform distribution.

We suppose that the N points $\{\mathbf{c}_k\}_{k=1}^N$ on the surface of the unit sphere are randomly placed according to a uniform distribution.

A virus enters the cell at the cellular membrane at a position uniformly distributed on the surface of the sphere of radius R. The virus then moves by pure diffusion with diffusion coefficient D in the three-dimensional cytoplasm (with a reflecting boundary condition at the cellular membrane at radius R) until it either hits the nucleus at radius δ or hits one of the N microtubules. If the virus ever reaches radius δ, then it is immediately absorbed. If the virus hits a microtubule, then it moves along the microtubule toward the nucleus with constant velocity V for an exponentially distributed amount of time. After this exponential time, the virus is released back into the cytoplasm at its current radius at a position uniformly distributed on the surface of the sphere with that radius, and then the virus begins to diffuse in the three-dimensional cytoplasm again.

The virus continues to alternate between epochs of diffusion and directed motion along microtubules until it reaches the nucleus. If we let $r_t \in [\delta, R]$ denote the radial position of the virus at time t, then the radial viral motion is described by

$$dr_t = \begin{cases} -V\,dt & \text{on a microtubule} \\ (2D/r_t)dt + \sqrt{2D}\,dW_t & \text{in cytoplasm.} \end{cases} \tag{4.1}$$

A. Coarse-grained spherical dynamics

To derive an effective SDE for the intermittent dynamics in Eq. (4.1), we cast the problem in the framework and notation of Sec. III. Let r_t denote the radial position of the virus and let $\mathbf{x}_t \in \mathbb{R}^3$ denote its Cartesian coordinates. Define the (ρ_t, ϕ_t) of Sec. III to be

$$(\rho_t, \phi_t) = (r_t, \mathbf{x}_t) \in \mathbb{R} \times \mathbb{R}^3.$$

The partitioning sets become

$$A_1 = \cup_{k=1}^N m_k \quad \text{and} \quad A_2 = \mathbb{R}^3 \backslash A_1.$$

The drift and diffusion terms become

$$b_1(\rho) = -V, \quad \sigma_1(\rho) = 0,$$
$$b_2(\rho) = 2D/\rho, \quad \sigma_2(\rho) = \sqrt{2D}.$$

In order to apply the method of Sec. III, it remains to approximate the process

$$1_{\phi_t \in A_1} + 21_{\phi_t \in A_2}$$

by a continuous-time Markov jump process J_t on $\{1,2\}$. Since the virus is assumed to attach to a microtubule for an exponential amount of time (say with mean μ), we suppose J_t jumps from state 1 to 2 with rate $1/\mu$.

Choosing the jump rate from state 2 to 1 is more difficult as it represents the rate at which a virus finds a microtubule. We choose it to be the inverse of the MFPT of a particle diffusing on the surface of a sphere to one of the N microtubules.

More precisely, let S denote the surface of the unit sphere and let $\eta(\rho) \subset S$ denote the set

$$\eta(\rho) := \{\mathbf{x} \in S : |\mathbf{x} - \mathbf{c}_k| \leqslant \varepsilon/\rho \quad \text{for some} \quad k = 1, \ldots, N\}.$$

Suppose $\tau(\mathbf{x}; \rho) : S \to [0, \infty)$ satisfies the following boundary value problem:

$$\Delta\tau(\mathbf{x}; \rho) = -\rho^2/D, \quad \mathbf{x} \in S\backslash\eta(\rho),$$
$$\tau(\mathbf{x}; \rho) = 0, \quad \mathbf{x} \in \partial\eta(\rho).$$

For a particle diffusing with diffusion coefficient D on the surface of a sphere of radius ρ, the quantity

$$\frac{1}{4\pi} \int_S \tau(\mathbf{x}; \rho)\, d\mathbf{x} \tag{4.2}$$

is the MFPT to hit one of N traps of radius ε centered at positions $\{\rho\mathbf{c}_k\}_{k=1}^N$, assuming the particle is initially distributed uniformly. Coombs, Straube, and Ward provide the following asymptotic approximation of Eq. (4.2) in the small ε limit [20]:

$$T(\rho) := \frac{\rho^2}{D}\left[-\frac{2}{N}\ln\left(\frac{\varepsilon}{\rho}\right) + 2\ln 2 - 1 - \frac{4}{N^2}\Psi\right],$$

where

$$\Psi = \sum_{k=1}^N \sum_{j>k}^N \ln|\mathbf{c}_k - \mathbf{c}_j|.$$

If we choose the jump rate of J_t from state 2 to 1 to be $1/T(\rho)$, then the quasi steady state distribution of J_t is given by

$$p_1(\rho) = \frac{\mu}{\mu + T(\rho)},$$

with $p_2(\rho) = 1 - p_1(\rho)$.

Thus, using Eq. (3.2) in Sec. III, we approximate the intermittent dynamics in Eq. (4.1) by the following effective SDE:

$$d\rho_t = \left(\frac{2D}{\rho_t}\frac{T(\rho_t)}{\mu + T(\rho_t)} - V\frac{\mu}{\mu + T(\rho_t)}\right)dt + \sqrt{2D\frac{T(\rho_t)}{\mu + T(\rho_t)}}\,dW_t. \tag{4.3}$$

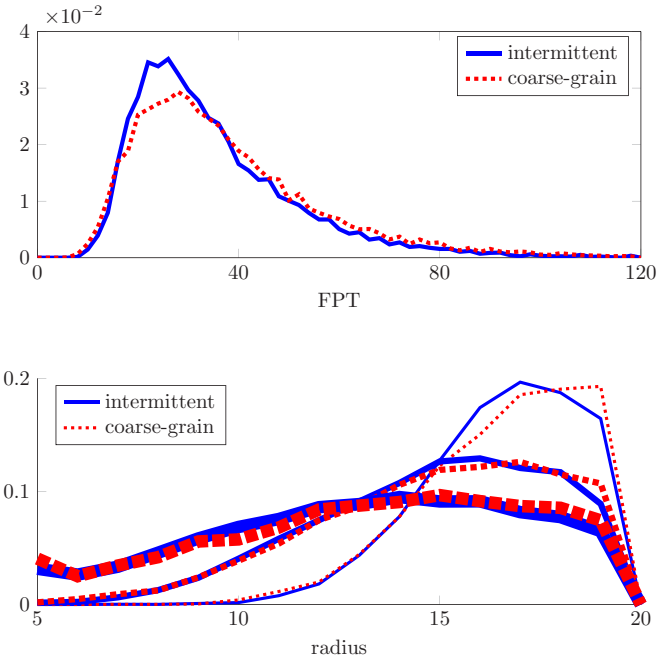

FIG. 6. (Color online) 3D spherical cell: comparison of intermittent in Eq. (4.1) and our coarse grain in Eq. (4.3). Each distribution is calculated from 10^4 trials and parameters are given in Sec. IV B. Top: Empirical distributions of FPT to nucleus. Bottom: Empirical distribution of radial position at times $t = 5, 10, 15$. Thicker lines correspond to larger times.

B. Comparison

We now compare the 3D intermittent dynamics of Eq. (4.1) to our effective SDE in Eq. (4.3).

In keeping with the parameters used in Sec. II, we take the radius of the cell to be $R = 20\ \mu$m, the radius of the nucleus to be $\delta = 5\ \mu$m, the cytoplasmic diffusion coefficient to be $D = 1.3\ \mu\text{m}^2\,\text{s}^{-1}$, the velocity on microtubules to be $V = 0.7\ \mu\text{m}\,\text{s}^{-1}$, and the average time on a microtubule to be $\mu = 1$ s. A typical eukaryotic cell large aster has between 600 and 1000 microtubules [16], and so we take $N = 1000$. A microtubule has approximate diameter 0.03 μm [21], an Adeno associated virus has approximate diameter 0.03 μm [5], and the interaction range between microtubules and molecular motors is approximately 0.05 μm [17]. Thus, we take $\varepsilon = 0.1\ \mu$m. The standard Euler-Maruyama method is used to simulate the cytoplasmic motion in the intermittent process as well as the effective SDE.

The top of Fig. 6 compares the distributions of the FPT to the nucleus and the bottom compares the distributions of the radial positions at a sequence of times. That is, the bottom compares the distribution of r_t for Eqs. (4.1) and (4.3) at $t = 5, 10, 15$. In both cases, the coarse-grained SDE closely approximates the full intermittent dynamics.

V. THREE-DIMENSIONAL CELL—CYLINDER

In this section, we formulate a mathematical model of virus trafficking in a three-dimensional cylindrical cell and apply our general coarse-graining method of Sec. III to derive an effective SDE describing viral motion. This cylindrical geometry is well motivated as many viruses rely on trafficking though axons and dendrites which resemble long cylinders.

Indeed, similar mathematical models of axonal transport have a long and rich history. Following experimental work in the 1970s and 1980s that showed radiolabeled amino acids progressing through axons as slowly spreading waves, Reed and Blum developed PDE models of axonal transport that remarkably exhibited this same behavior [22–24]. These PDE models have been generalized and have generated lots of rigorous mathematical analysis [25–28]. In addition to PDE models, probabilistic models (in both discrete and continuous time) have been constructed that also demonstrate this same behavior [29–32].

These previous models begin with two simplifying reductions: (a) the cell is one-dimensional, and (b) the rate at which a virus (or other cargo) attaches to a microtubule is some given exponential rate. Our intermittent model makes neither reduction; the cell's three-dimensional geometry is included, and the time when a virus attaches to a microtubule is determined by the random time that a virus diffusing in the three-dimensional cytoplasm hits a microtubule. However, the coarse-grained SDE that we derive in Sec. V A does make use of these reductions. We show in Sec. V B that this SDE compares favorably with the full intermittent model, and therefore verify the efficacy of these reductions and show how to make them. That is, we show how to choose the pair of one-dimensional parameters (drift and diffusion coefficient) in order to encapsulate the full three-dimensional model.

We now define the intermittent dynamics. In this model, the cell is a cylinder of length L and radius R:

$$C := \{(x,y,z) \in \mathbb{R}^3 : 0 \leqslant x \leqslant L \text{ and } y^2 + z^2 \leqslant R^2\}.$$

There are N microtubules, each of radius ε and length L, that run parallel to the principal axis of the cell (see Fig. 7). More precisely, for N points $\{(y_k,z_k)\}_{k=1}^N$ on the disk of radius R in the (y,z) plane, we define the microtubules $\{m_k\}_{k=1}^N$ to be the sets

$$m_k = \{(x,y,z) \in \mathbb{R}^3 : 0 \leqslant x \leqslant L,\ |(y,z) - (y_k,z_k)| \leqslant \varepsilon\}.$$

We suppose the N points $\{(y_k,z_k)\}_{k=1}^N$ are randomly placed on the disk of radius R according to a uniform distribution.

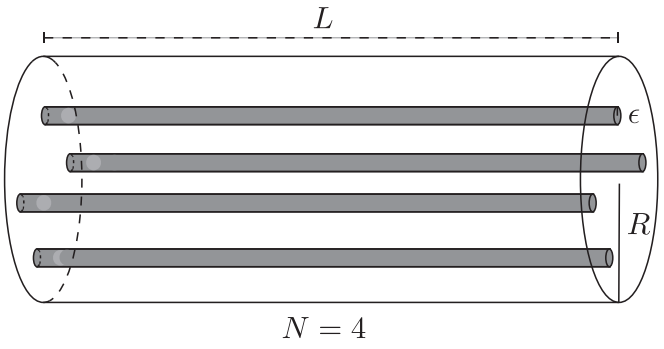

FIG. 7. Three-dimensional cylindrical (axon) model with cell radius R, length L, and $N = 4$ microtubules with radius ε. The locations of the N microtubules are randomly drawn from a uniform distribution.

We suppose that a virus enters the cell at position $(0,y_0,z_0) \in C$ with (y_0,z_0) uniformly distributed on the disk of radius R. The virus then moves by pure diffusion with diffusion coefficient D in the three-dimensional cytoplasm with a reflecting boundary condition at the cellular membrane

$$\{(y,z) \in \mathbb{R}^2 : y^2 + z^2 = R^2\}$$

and at the left end of the cell ($x = 0$), until it either hits the right end of the cell ($x = L$) or hits one of the N microtubules. If the virus reaches $x = L$, then it is immediately absorbed. If the virus hits a microtubule, then it moves along the microtubule with constant velocity $V > 0$ for an exponentially distributed amount of time. After this exponential time, the virus is released back into the cytoplasm at its current x position at a point in the (y,z) plane uniformly distributed on the disk of radius R, and then the virus begins to diffuse again.

The virus continues to alternate between epochs of diffusion and directed motion along microtubules until it reaches $x = L$. If we let $(x_t,y_t,z_t) \in C$ denote the position of the virus at time t, then the viral motion in the x direction is described by

$$dx_t = \begin{cases} V\,dt & \text{on a microtubule} \\ \sqrt{2D}\,dW_t & \text{in cytoplasm.} \end{cases} \tag{5.1}$$

A. Coarse-grained cylindrical dynamics

To derive an effective SDE for the intermittent dynamics in Eq. (5.1), we cast the problem in the framework and notation of Sec. III. Define the (ρ_t,ϕ_t) of Sec. III to be

$$(\rho_t,\phi_t) = (x_t,(y_t,z_t)) \in C.$$

The partitioning sets become

$$A_1 = \cup_{k=1}^{N} m_k \quad \text{and} \quad A_2 = C \backslash A_1.$$

The drift and diffusion terms become

$$b_1(\rho) = V, \quad \sigma_1(\rho) = 0,$$
$$b_2(\rho) = 0, \quad \sigma_2(\rho) = \sqrt{2D}.$$

In order to apply the method of Sec. III, it remains to approximate the process

$$1_{\phi_t \in A_1} + 21_{\phi_t \in A_2}$$

by a continuous-time Markov jump process J_t on $\{1,2\}$. Since the virus is assumed to attach to a microtubule for an exponential amount of time (say with mean μ), we suppose J_t jumps from state 1 to state 2 at rate $1/\mu$.

The jump rate from state 2 to state 1 represents the rate at which a virus finds a microtubule. We choose it to be the inverse of the MFPT of a particle diffusing on the disk of radius R to one of N uniformly distributed circular traps of radius ε. In the small ε limit, this MFPT is Ref. [9]

$$T = \frac{R^2 \ln(1/\varepsilon)}{2ND}.$$

The quasi steady state distribution of J_t is then given by

$$p_1 = \frac{\mu}{\mu + T} \quad \text{and} \quad p_2 = \frac{T}{\mu + T}.$$

Thus, using Eq. (3.2) in Sec. III, we approximate the intermittent dynamics in Eq. (5.1) by the following effective SDE:

$$d\rho_t = V\frac{\mu}{\mu + T}\,dt + \sqrt{2D\frac{T}{\mu + T}}\,dW_t. \tag{5.2}$$

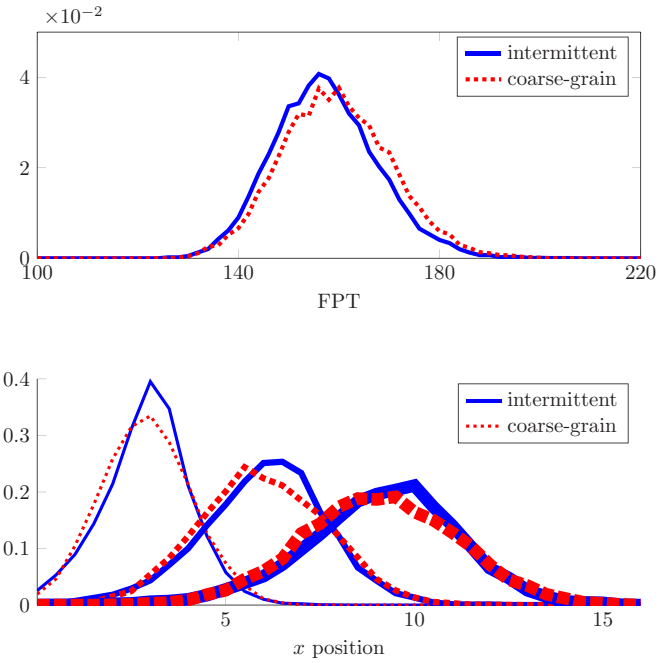

FIG. 8. (Color online) 3D cylindrical cell: comparison of intermittent in Eq. (5.1) and our coarse grain in Eq. (5.2). Each distribution is calculated from 10^4 trials and parameters are given in Sec. V B. Top: Empirical distributions of FPT to nucleus. Bottom: Empirical distribution of x position at times $t = 5,10,15$. Thicker lines correspond to larger times.

B. Comparison

We now compare the 3D intermittent dynamics of Eq. (5.1) to our effective SDE in Eq. (5.2). As above, we take $\varepsilon = 0.1\ \mu$m, $D = 1.3\ \mu\text{m}^2\,\text{s}^{-1}$, $V = 0.7\ \mu\text{m}\,\text{s}^{-1}$, and $\mu = 1$ s. We take $R = 10\ \mu$m, $L = 100$, and $N = 700$ [33,34]. The standard Euler-Maruyama method is used to simulate the cytoplasmic motion in the intermittent process as well as the effective SDE.

The top of Fig. 8 compares distributions of the FPT to $x = L$ and the bottom compares the distributions of the x positions at a sequence of times. That is, the bottom compares x_t in Eq. (5.1) and ρ_t in Eq. (5.2) at $t = 5,10,15$. In both cases, the coarse-grained SDE closely approximates the full intermittent dynamics.

VI. SUMMARY AND CONCLUSIONS

In this paper, we developed a method for coarse-graining intermittent intracellular transport into effective SDEs. We used Monte Carlo simulations to demonstrate the accuracy of our method across a variety of cellular geometries. For comparison and analogy to previous work, we incorporated various assumptions into the intermittent models (deterministic motion on microtubules, uniform placement in cytoplasm

after leaving a microtubule, etc.). However, we stress that our method (as described in Sec. III) is easily applied without these assumptions. We anticipate our method being used on future intermittent models and the machinery of Ref. [11] being applied to our effective SDEs [Eqs. (2.6) and (4.3)] to estimate the efficiency of viral infection. Additional future work includes combining our present coarse-grained models of viral motion with the sequence of biochemical transformations that viruses undergo during their journey through the cell, as these are known to affect the probability and timing of infection [35].

ACKNOWLEDGMENTS

We thank Paul C. Bressloff for comments on this work. S.D.L. was supported by NSF Grant No. DMS-RTG 1148230, M.T. was supported by NSF Grant No. DMS-RTG 1148230, and H.A.B. was supported by NSF Grant No. DMS-RTG 1148230.

[1] M. Aridor and L. A. Hannan, Traffic **1**, 836 (2000).
[2] C. M. Wiethoff and C. R. Middaugh, J. Pharm. Sci. **92**, 203 (2003).
[3] G. Zuber, E. Dauty, M. Nothisen, P. Belguise, and J.-P. Behr, Adv. Drug Delivery Rev. **52**, 245 (2001).
[4] K. Dohner, C.-H. Nagel, and B. Sodeik, Trends Microbiol. **13**, 320 (2005).
[5] G. Seisenberger, M. U. Ried, T. Endress, H. Buning, M. Hallek, and C. Brauchle, Science **294**, 1929 (2001).
[6] N. Arhel, A. Genovesio, K.-A. Kim, S. Miko, E. Perret, J.-C. Olivo-Marin, S. Shorte, and P. Charneau, Nat. Methods **3**, 817 (2006).
[7] B. Brandenburg and X. Zhuang, Nat. Rev. Microbiol. **5**, 197 (2007).
[8] T. Lagache and D. Holcman, SIAM J Appl. Math. **68**, 1146 (2008).
[9] T. Lagache and D. Holcman, Phys. Rev. E **77**, 030901(R) (2008).
[10] P. C. Bressloff and J. M. Newby, Rev. Mod. Phys. **85**, 135 (2013).
[11] D. Holcman, J. Stat. Phys. **127**, 471 (2007).
[12] T. Lagache, E. Dauty, and D. Holcman, Phys. Rev. E **79**, 011921 (2009).
[13] T. Lagache, E. Dauty, and D. Holcman, Curr. Opin. Microbiol. **12**, 439 (2009).
[14] A.-T. Dinh, T. Theofanous, and S. Mitragotri, Biophys. J. **89**, 1574 (2005).
[15] S. Redner, *A Guide to First-Passage Processes* (Cambridge University Press, Cambridge, UK, 2001).
[16] F. Nedelec, T. Surrey, and A. C. Maggs, Phys. Rev. Lett. **86**, 3192 (2001).
[17] D. L. Coy, M. Wagenbach, and J. Howard, J. Biol. Chem. **274**, 3667 (1999).
[18] S. J. King and T. A. Schroer, Nat. Cell Biol. **2**, 20 (2000).
[19] G. G. Yin and C. Zhu, *Hybrid Switching Diffusions: Properties and Applications* (Springer Science & Business Media, Berlin-Heidelberg, 2009).
[20] D. Coombs, R. Straube, and M. Ward, SIAM J. Appl. Math. **70**, 302 (2009).
[21] F. Gittes, B. Mickey, J. Nettleton, and J. Howard, J. Cell Biol. **120**, 923 (1993).
[22] J. J. Blum and M. C. Reed, Cell Motil. **5**, 507 (1985).
[23] M. C. Reed and J. J. Blum, Cell Motil. Cytoskeleton **6**, 620 (1986).
[24] M. C. Reed, S. Venakides, and J. J. Blum, SIAM J. Appl. Math. **50**, 167 (1990).
[25] A. Friedman and G. Craciun, J. Math. Biol. **51**, 217 (2005).
[26] A. Friedman and G. Craciun, SIAM J. Math. Anal. **38**, 741 (2006).
[27] A. Friedman and B. Hu, Indiana Univ. Math. J. **56**, 2133 (2007).
[28] A. Friedman and B. Hu, Arch. Ration. Mech. Anal. **186**, 251 (2007).
[29] E. A. Brooks, Ann. Appl. Probab. **9**, 719 (1999).
[30] P. C. Bressloff, Phys. Rev. E **74**, 031910 (2006).
[31] P. Bressloff and J. Newby, New J. Phys. **11**, 023033 (2009).
[32] L. Popovic, S. A. McKinley, and M. C. Reed, SIAM J. Appl. Math. **71**, 1531 (2011).
[33] D. Debanne, E. Campanac, A. Bialowas, E. Carlier, and G. Alcaraz, Physiol. Rev. **91**, 555 (2011).
[34] W. Yu and P. W. Baas, J. Neurosci. **14**, 2818 (1994).
[35] M. R. D'Orsogna and T. Chou, PLoS ONE **4**, e8165 (2009).